cm^{-1}) was assigned to the more strongly bound BH_3CN^- group (i.e. the shorter Cu–N bond), which has a nonlinear Cu–N–C unit (with the longer of the two C–N bonds). The ν_{CN} with the larger shift (31 cm^{-1}) was assigned to the more weakly bound BH_3CN^-, which contains a linear Cu–N–C unit.

In $CoH(BH_3CN)(PPh_3)_3$, the Co–N–C unit is linear, the Co–N bond length is shorter than either of the two Cu–N bond lengths in the above-mentioned Cu compound, and the C–N bond is longer than in most other coordinated or uncoordinated $-C\equiv N$ linkages.[9] It is difficult, therefore, to account for a shift in ν_{CN} of only 11 cm^{-1} in the spectrum of this cobalt complex, and clearly, correlations between ν_{CN} and such features as the M–N–C angle and the M–N bond strength in $M-NCBH_3$ complexes should be made with caution.

No solution spectroscopic or magnetic studies could be carried out for $CoH(BH_3CN)(PPh_3)_3$ because of its very rapid decomposition in most solvents, even at −70 °C. However, in the solid state, the complex contains low-spin Co(II) (μ_{eff} = 1.9 μ_B), as does the related[5] $CoH(BH_4)(PCy_3)_2$ previously mentioned, and this is consistent with a strong interaction between the Co and H atoms.

Acknowledgment. The authors thank the Natural Sciences and Engineering Research Council of Canada for financial support in the form of operating grants to R.J.B. and B.E.R. and to D.G.H. and A.N.H. We also thank the University of Xiamen for research leave granted to H.S.

Registry No. $CoH(BH_3CN)(PPh_3)_3$, 90605-24-6.

Supplementary Material Available: Table A, observed and calculated structure amplitudes, Table B, anisotropic temperature factors, and a stereoscopic view of the molecule $CoH(BH_3CN)(PPh_3)_3$ (15 pages). Ordering information is given on any current masthead page.

Contribution from the J. D. McCullough Laboratory for X-ray Crystallography, Department of Chemistry and Biochemistry, University of California, Los Angeles, California 90024

Two-Dimensional Short-Range Order in the Crystal Structure of (Tetraphenylporphinato)iron(III) 2,3,5,6-Tetrafluorobenzenethiolate. Analysis of the X-ray Diffuse Scattering and a Simulation of Crystal Growth

KATHLEEN M. MILLER and CHARLES E. STROUSE*

Received September 2, 1983

The five-coordinate iron porphyrin complex (tetraphenylporphinato)iron(III) 2,3,5,6-tetrafluorobenzenethiolate, Fe(TPP)(SC_6HF_4), crystallizes in the monoclinic space group $P2_1/a$ with a = 13.272 (4) Å, b = 12.685 (6) Å, c = 22.46 (1) Å, β = 97.17 (3)°, and Z = 4. The iron atom is displaced 0.395 (3) Å from the plane of the four nitrogen atoms, and the Fe–S distance is 2.298 (3) Å. The hkl, $k + l = 2n + 1$, reflections are observed to be diffuse. The diffuse intensity is in the form of circular disks perpendicular to the a^* axis, indicating a lack of long-range order in the **b** and **c** directions. The specific nature of the disorder has been deduced, and potential mechanisms for its introduction have been examined in two-dimensional simulations of the crystal growth.

Recent investigations in this laboratory have focused on sulfur-ligated ferric porphyrin complexes. Single-crystal ESR and X-ray techniques have been used to characterize the electronic structure of these species and to provide quantitative descriptions of the axial ligand binding.[1-3] A series of isomorphous thiol/thiolate complexes displaying spin-state and structural equilibria in the solid state has been prepared. In this series, the free energy change associated with a structural transformation is strongly influenced by the σ-donor strength of the axial ligand. In an effort to extend the range of σ-donor strengths examined, syntheses of (tetraphenylporphinato)iron(III) complexes with the axial ligand 2,3,5,6-tetrafluorobenzenethiol have been undertaken. Isolated in the course of these syntheses was the five-coordinate thiolate complex Fe(TPP)(SC_6HF_4) (I),[4] which is the subject of this report. Crystals of this material exhibit a relatively unusual kind of two-dimensional short-range order, the nature of which has been deduced from the observed diffuse scattering. The disorder in this structure has been mimicked in a two-dimensional simulation of the crystal growth.

Table I. Crystallographic Data

formula	$FeSN_4C_{56}H_{31}F_4$
cryst dimens, mm	0.15 × 0.20 × 0.35
space group	$P2_1/a$
Z	4
a, Å	13.272 (4)
b, Å	12.685 (6)
c, Å	22.46 (1)
β, deg	97.17 (3)
vol, $Å^3$	3752 (3)
density (calcd), g/cm^3	1.50
radiation, Å	Mo Kα (0.7107), cryst monochromatized
temp, K	117
scan range	$1° < K\alpha_1$ to $1° > K\alpha_2$
scan rate, deg/min	2.0
scan mode	$\theta/2\theta$
2θ max, deg	45
unique data	5453
reflctns ($I > 3\sigma(I)$)	1554 ($k + l = 2n$, only)
μ, cm^{-1}	5.157
transmission factors	0.82–0.94
data collcd	$+h,+k,\pm l$
R	0.078
R_w	0.088
erf	2.25
no. of params refined	159

(1) Byrn, M. P.; Katz, B. A.; Keder, N. L.; Levan, K. R.; Magurany, C. J.; Miller, K. M.; Pritt, J. W.; Strouse, C. E. *J. Am. Chem. Soc.* **1983**, *105*, 4916.
(2) Byrn, M. P.; Strouse, C. E. *J. Am. Chem. Soc.* **1981**, *103*, 2633.
(3) Collman, J. P.; Sorrell, T. N.; Hodgson, K. O.; Kulshrestha, A. K.; Strouse, C. E. *J. Am. Chem. Soc.* **1977**, *99*, 5180.
(4) Abbreviations used: TPP, tetraphenylporphyrin dianion; SC_6HF_4, 2,3,5,6-tetrafluorobenzenethiolate; PPIXDME, protoporphyrin IX dimethyl ester dianion; SC_6H_4-*p*-NO_2, *p*-nitrobenzenethiolate.

0020-1669/84/1323-2395$01.50/0

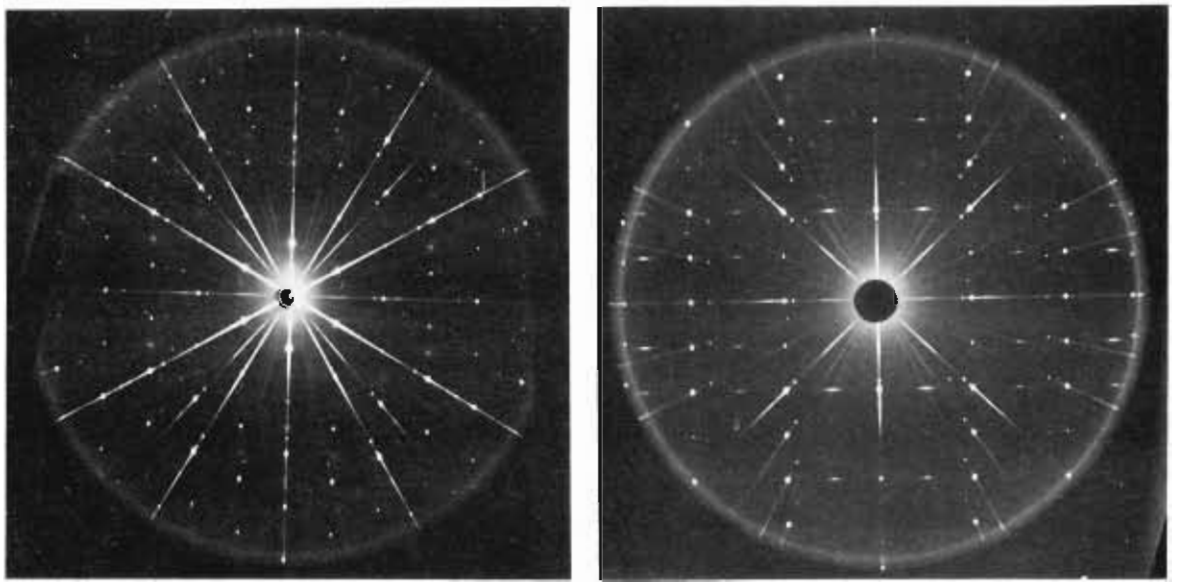

a b

Figure 1. Precession photographs of (a) the b^*c^* plane with the b^* axis horizontal and the c^* axis vertical and (b) the a^*b^* plane with the b^* axis horizontal and the a^* axis vertical.

Experimental Section

Preparation of Compounds. All syntheses were conducted under a dinitrogen atmosphere. $Fe(OAc)_2$[5] and $[Fe(TPP)]_2O$[6] were prepared by published methods.

Fe(TPP)(SC_6HF_4) (I). To a solution of 52.5 mg (0.039 mmol) of $[Fe(TPP)]_2O$ in 20 mL of benzene was added 20 mL of 15% (v/v) aqueous sulfuric acid with rapid stirring. After 1 h, 100 μL (0.83 mmol) of 2,3,5,6-tetrafluorobenzenethiol (Aldrich) was added, and the solution was left to stir for 1 h. The organic phase was separated and allowed to evaporate to near dryness. A mixture of small purple crystals and an amorphous purple precipitate resulted.

X-ray Data Collection. A Syntex $P\bar{1}$ diffractometer equipped with a variable-temperature device[7] was used to obtain the diffraction data. The cell constants and other crystallographic data are reported in Table I. Three standard reflections were measured every 97 reflections and showed no appreciable decay. The data were corrected for absorption.

Solution and Refinement of the Structure. Inspection of the intensity data revealed the systematic absences $0k0$, $k = 2n + 1$, and $h0l$, $h = 2n + 1$, consistent with the space group $P2_1/a$, a nonstandard setting of $P2_1/c$. The iron atom was located by direct methods (MULTAN78), and the positions of the non-hydrogen tetraphenylporphyrin atoms and the axial sulfur atom were found by successive cycles of full-matrix least-squares refinement and difference-Fourier syntheses.[8] Positions for the tetrafluorobenzene ring of the axial ligand were calculated from the positions of the sulfur atom and two phenyl carbon atoms. Refinement was continued to convergence at $R = 0.30$.

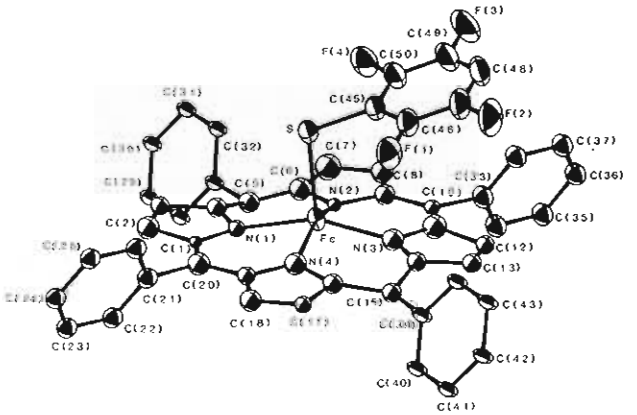

Figure 2. Molecular structure of Fe(TPP)(SC_6HF_4) showing the numbering scheme (50% probability ellipsoids). Hydrogen atoms and selected atom labels have been omitted for clarity.

A difference map revealed a peak approximately 1.0 Å from the iron atom on the opposite side of the porphyrin plane, suggesting a disorder of the Fe–SC_6HF_4 moiety. It was also observed that the set of reflections hkl, $k + l = 2n + 1$, had $F_o < F_c$ and those with hkl, $k + l = 2n$, had $F_o > F_c$. The crystal was remounted along the b axis, and precession photographs were obtained of the $hk0$ and $0kl$ zones (see Figure 1). These photographs reveal that the $k + l = 2n + 1$ reflections are diffuse; the diffuse intensity is in the form of circular disks extending in the bc plane. This observation is characteristic of "linear" disorder;[9] i.e., the long range periodicity of the lattice is preserved in only the **a** direction (vide infra).

Only the $k + l = 2n$ reflections, those insensitive to the inversion disorder, were included in the final stages of the least-squares refinement. To maximize the data to parameter ratio, the porphyrin phenyl rings and the tetrafluorobenzenethiolate ligand were refined with idealized geometries.[10] Parameters corresponding to the C–C and C–H distances of the porphyrin phenyl groups were refined;[11]

(5) Hardt, H.; Moller, W. *Z. Anorg. Allg. Chem.* **1961**, *313*, 57.
(6) Adler, A. D.; Longo, F. R.; Kampas, F.; Kim, J. *J. Inorg. Nucl. Chem.* **1970**, *32*, 2443.
(7) Strouse, C. E. *Rev. Sci. Instrum.* **1976**, *47*, 871.
(8) The programs used in this work included modified versions of the following: CARESS (Broach; includes the program PROFILE (Coppens, Becker, and Blessing)), peak profile analysis, Lorentz and polarization corrections; MULTAN (Main), package of programs, including direct methods, structure factor normalization, Fourier transform, and peak search; ORFLS (Busing, Martin, and Levy), structure factor calculation and full-matrix, least-squares refinement; ORFFE (Busing, Martin, and Levy), distance, angle, and error calculations; ABSORB (Coppens; Edwards and Hamilton), absorption correction calculation; ORTEP (Johnson), figure plotting; HYDROGEN (Trueblood), calculation of hydrogen atom positions. All least-squares refinements computed the agreement factors R and R_w according to

$$R = (\sum||F_o| - |F_c||/\sum|F_o|) \qquad R_w = (\sum w||F_o| - |F_c||^2/\sum w|F_o|^2)^{1/2}$$

where F_o and F_c are the observed and calculated structure factors, respectively, and $w = 1/\sigma^2(F_o)$. All calculations were performed on a DEC VAX 11/780 departmental computer. Scattering factors and corrections for anomalous dispersion were taken from: "International Tables for X-Ray Crystallography"; Kynoch Press: Birmingham, England, 1974; Vol. IV.
(9) Guinier, A. "X-Ray Diffraction"; W. H. Freeman: San Francisco, CA, 1963; p 179.
(10) Strouse, C. E. *Acta. Crystallogr., Sect. A.* **1970**, *A26*, 604.
(11) Porphyrin phenyl group distances: C(5)–C(27), 1.50 Å; C(10)–C(33), 1.46 Å; C(15)–C(39), 1.53 Å; C(20)–C(21), 1.57 Å; C–H, 0.98 Å. Tetrafluorobenzenethiolate group distances: S–C, 1.79 Å; C–F 1.31 Å; C–H, 0.77 Å.

Table II. Positional Parameters with Estimated Standard Deviations for the Atoms in Fe(TPP)(SC_6HF_4)

atom	x	y	z
Fe	0.9649 (2)	0.2683 (2)	0.7364 (1)
	Porphyrin Core Atoms		
C(1)	1.0131 (13)	0.1057 (15)	0.6403 (9)
C(2)	1.0456 (21)	0.1066 (23)	0.5821 (12)
C(3)	1.0793 (16)	0.2016 (17)	0.5705 (10)
C(4)	1.0736 (17)	0.2648 (19)	0.6232 (10)
C(5)	1.1220 (17)	0.3611 (20)	0.6409 (11)
C(6)	1.0934 (23)	0.4305 (26)	0.6802 (14)
C(7)	1.1178 (21)	0.5375 (24)	0.6840 (13)
C(8)	1.0924 (21)	0.5725 (24)	0.7393 (13)
C(9)	1.0538 (18)	0.4893 (20)	0.7652 (11)
C(10)	1.0207 (16)	0.4905 (18)	0.8217 (10)
C(11)	0.9749 (18)	0.4090 (20)	0.8457 (11)
C(12)	0.9509 (19)	0.4102 (20)	0.9084 (11)
C(13)	0.9066 (16)	0.3124 (18)	0.9172 (10)
C(14)	0.9121 (16)	0.2505 (18)	0.8663 (10)
C(15)	0.8973 (17)	0.1352 (19)	0.8708 (10)
C(16)	0.8950 (22)	0.0796 (24)	0.8117 (13)
C(17)	0.8652 (18)	−0.0322 (19)	0.8059 (11)
C(18)	0.8908 (21)	−0.0664 (24)	0.7526 (13)
C(19)	0.9358 (17)	0.0243 (19)	0.7230 (10)
C(20)	0.9699 (20)	0.0217 (21)	0.6665 (12)
N(1)	1.0290 (12)	0.2025 (13)	0.6639 (8)
N(2)	1.0497 (11)	0.3988 (12)	0.7290 (7)
N(3)	0.9520 (13)	0.3061 (14)	0.8223 (8)
N(4)	0.9336 (13)	0.1118 (15)	0.7576 (8)
	Axial Thiolate Ligand Group Atoms		
S	0.8156	0.3218	0.6818
C(45)	0.7643	0.4141	0.7303
C(46)	0.7146	0.3781	0.7775
C(47)	0.6746	0.4500	0.8153
C(48)	0.6843	0.5580	0.8058
C(49)	0.7340	0.5941	0.7585
C(50)	0.7740	0.5222	0.7208
F(1)	0.7055	0.2768	0.7864
F(2)	0.6279	0.4162	0.8596
H(48)	0.6622	0.5978	0.8267
F(3)	0.7431	0.6954	0.7496
F(4)	0.8206	0.5560	0.6764

the diagonal elements of the group translational vibration tensor, T, were refined for each of these groups.[12] For the tetrafluorobenzenethiolate group, the origin was chosen at the sulfur atom and the S–C(phenyl), C–F, and C–H distances were refined,[11] along with the diagonal elements of both the group translational vibration tensor, T, and the group libration tensor, L. Anisotropic thermal parameters were refined for the iron atom. Individual isotropic temperature factors were refined for the non-group, non-hydrogen atoms of the porphyrin core. The hydrogen atom positions for the pyrrole carbons were calculated (C–H = 1.00 Å) and not changed through the course of refinement. Their isotropic temperature factors were set to 3.0 $Å^2$. The largest features in a final difference map were two peaks of height 1.2 e/$Å^3$. One of these peaks was located between the iron and the sulfur atoms and the other between a fluorine atom in the ortho position of the thiolate ligand and the iron atom of an adjacent molecule. The refinement converged with final R factors $R = 0.078$ and $R_w = 0.088$. Atomic positions are presented in Table II, and a summary of bond distances and angles is given in Table III. The numbering scheme used is shown in Figure 2. Thermal parameters (Table I-S), porphyrin hydrogen atom positions (Table II-S), porphyrin group atom positions (Table III-S), and a listing of observed and calculated structure factor amplitudes are available in the supplementary material.

Results and Dicussion

The Molecular Structure. Some caution must be exercised in the interpretation of the structural parameters obtained in this determination. Omission of the $k + l = 2n + 1$ reflections together with the pseudo-A-centering (vide infra) leads to some large correlations (maximum 0.91) in the refinement, particularly among parameters of those atoms of the porphyrin ligand related by the pseudoinversion center. Examination of the thermal parameters depicted in Figure 2 reveals evidence of the consequence of these correlations.

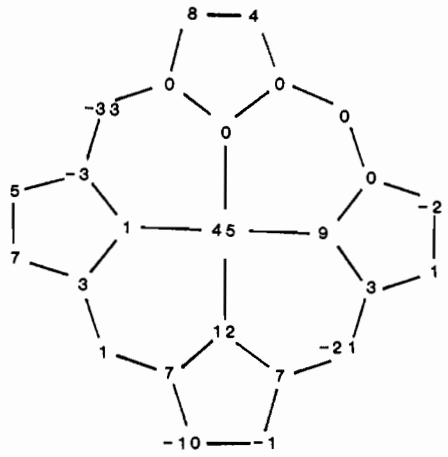

Figure 3. Perpendicular displacement of atoms, in units of 0.01 Å, from the least-squares plane of the 24-atom porphyrin core.

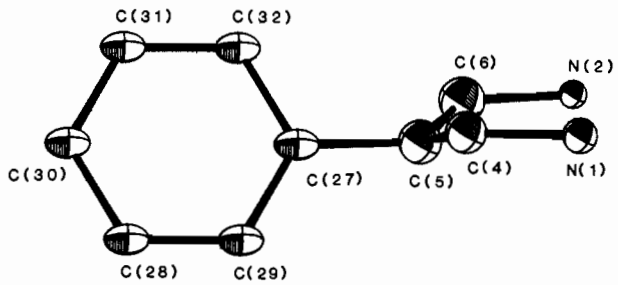

Figure 4. The C(5)-phenyl moiety depicting the unusual deviation of C(5) from the porphyrin plane and the linearity of the C(5)–C(27)–C(30) atoms.

The bond distances and bond angles within the porphyrin core are similar to those of numerous reported tetraphenylporphyrin structures.[13] The FeN_4S moiety has the pyramidal structure found for five-coordinate, high-spin iron(III) porphyrin complexes.[13,14] The observed Fe–N distances range from 2.02 (2)[15] to 2.10 (2) Å but, because of their relatively large uncertainity, do not deviate significantly from the mean of 2.06 Å. The iron atom is displaced 0.452 (3) Å from the mean porphyrin plane and 0.395 (3) Å from the N_4 plane toward the axial thiolate ligand. These values are in the range reported for other five-coordinate iron(III) porphyrin complexes.[16] The distances of the 24 porphyrin core atoms and the iron atom from the least-squares plane are shown in Figure 3. The meso carbons C(5) and C(15) display unusually large displacements of 0.33 (2) and 0.21 (2) Å, respectively. The nearly linear arrangement of the C(5)–C(27)–C(30) atoms and the C(15)–C(39)–C(42) atoms, however, supports the significance of these displacements (see Figure 4). The mean Fe–N bond distance and the out-of-plane iron distances are similar to the corresponding distances reported for the five-coordinate iron(III) porphyrin thiolate complex, Fe-

(12) Schomaker, V.; Trueblood, K. N. *Acta. Crystallogr., Sect. B* **1968**, *B24*, 63.

(13) (a) Koenig, D. M. *Acta. Crystallogr.* **1965**, *18*, 663. (b) Hoard, J. L; Hamor, M. J.; Hamor, T. A.; Caughey, W. S. *J. Am. Chem. Soc.* **1965**, *87*, 2312. (c) Hoffman, A. B.; Collins, D. M.; Day, V. W.; Fleischer, E. B. *Ibid.* **1972**, *94*, 3620.

(14) (a) Hoard, J. L.; Cohen, G. H.; Glick, M. D. *J. Am. Chem. Soc.* **1967**, *89*, 1992. (b) Kazunori, A.; Hatano, K.; Lee, Y. J.; Scheidt, W. R. *Inorg. Chem.* **1981**, *20*, 2337.

(15) Values in parentheses are estimated standard deviations of the least significant digit for individual observations.

(16) (a) Hoard, J. L. *Science (Washington, D.C.)* **1971**, *174*, 1295. (b) Scheidt, W. R. *Acc. Chem. Res.* **1977**, *10*, 339. (c) Scheidt, W. R.; Reed, C. A. *Chem. Rev.* **1981**, *81*, 543.

Table III. Bond Distances (Å) and Interbond Angles (deg) in Fe(TPP)(SC_6HF_4), with Estimated Standard Deviations

Bond Distances

Fe-S	2.298 (5)	C(10)-C(11)	1.35 (3)
Fe-N(1)	2.10 (2)	C(14)-C(15)	1.48 (3)
Fe-N(2)	2.02 (2)	C(15)-C(16)	1.50 (4)
Fe-N(3)	2.02 (2)	C(1)-C(2)	1.43 (3)
Fe-N(4)	2.09 (2)	C(3)-C(4)	1.44 (3)
S-C(45)	1.79 (3)[a]	C(6)-C(7)	1.40 (4)
C(1)-N(1)	1.34 (2)	C(8)-C(9)	1.34 (4)
C(4)-N(1)	1.40 (3)	C(11)-C(12)	1.48 (3)
C(6)-N(2)	1.36 (3)	C(13)-C(14)	1.40 (3)
C(9)-N(2)	1.40 (3)	C(16)-C(17)	1.47 (4)
C(11)-N(3)	1.43 (3)	C(18)-C(19)	1.49 (4)
C(14)-N(3)	1.37 (3)	C(2)-C(3)	1.32 (4)
C(16)-N(4)	1.44 (3)	C(7)-C(8)	1.40 (4)
C(19)-N(4)	1.36 (3)	C(12)-C(13)	1.40 (3)
C(1)-C(20)	1.38 (3)	C(17)-C(18)	1.36 (4)
C(19)-C(20)	1.40 (3)	C(5)-C(27)	1.50 (3)
C(4)-C(5)	1.41 (3)	C(10)-C(33)	1.46 (3)
C(5)-C(6)	1.33 (4)	C(15)-C(39)	1.53 (3)
C(9)-C(10)	1.40 (3)	C(20)-C(21)	1.57 (3)

Bond Angles

N(1)-Fe-S	96.3 (5)	C(20)-C(1)-C(2)	126.0 (21)
N(2)-Fe-S	99.6 (5)	C(5)-C(4)-C(3)	130.0 (21)
N(3)-Fe-S	105.6 (5)	C(5)-C(6)-C(7)	126.8 (30)
N(4)-Fe-S	102.6 (5)	C(8)-C(9)-C(10)	124.6 (24)
Fe-S-C(45)	103.7	C(10)-C(11)-C(12)	122.3 (22)
N(3)-Fe-N(2)	89.9 (7)	C(13)-C(14)-C(15)	118.6 (20)
N(3)-Fe-N(4)	88.0 (7)	C(17)-C(16)-C(15)	120.4 (24)
N(3)-Fe-N(1)	157.9 (7)	C(20)-C(19)-C(18)	125.4 (23)
N(2)-Fe-N(4)	157.4 (7)	C(3)-C(2)-C(1)	109.6 (24)
N(2)-Fe-N(1)	88.8 (6)	C(2)-C(3)-C(4)	106.9 (21)
N(4)-Fe-N(1)	84.8 (7)	C(6)-C(7)-C(8)	106.5 (28)
C(1)-N(1)-Fe	127.6 (13)	C(9)-C(8)-C(7)	106.4 (27)
C(4)-N(1)-Fe	121.9 (14)	C(13)-C(12)-C(11)	105.7 (22)
C(6)-N(2)-Fe	127.2 (17)	C(14)-C(13)-C(12)	108.4 (20)
C(9)-N(2)-Fe	127.2 (14)	C(18)-C(17)-C(16)	107.0 (24)
C(11)-N(3)-Fe	122.1 (15)	C(17)-C(18)-C(19)	107.7 (24)
C(14)-N(3)-Fe	130.8 (15)	C(6)-C(5)-C(4)	126.8 (23)
C(19)-N(4)-Fe	128.8 (16)	C(11)-C(10)-C(9)	124.4 (22)
C(16)-N(4)-Fe	124.3 (17)	C(14)-C(15)-C(16)	113.1 (20)
N(1)-C(1)-C(20)	126.3 (18)	C(1)-C(20)-C(19)	124.6 (24)
N(1)-C(4)-C(5)	121.3 (20)	C(1)-N(1)-C(4)	108.5 (17)
C(5)-C(6)-N(2)	121.5 (27)	C(6)-N(2)-C(9)	103.6 (20)
C(10)-C(9)-N(2)	122.8 (21)	C(14)-N(3)-C(11)	106.8 (18)
C(10)-C(11)-N(3)	130.0 (21)	C(19)-N(4)-C(16)	106.7 (20)
N(3)-C(14)-C(15)	128.5 (20)	C(4)-C(5)-C(27)	107.8 (19)
N(4)-C(16)-C(15)	130.2 (24)	C(6)-C(5)-C(27)	117.7 (22)
N(4)-C(19)-C(20)	124.8 (23)	C(9)-C(10)-C(33)	119.2 (20)
N(1)-C(1)-C(2)	107.7 (18)	C(11)-C(10)-C(33)	116.3 (21)
N(1)-C(4)-C(3)	107.1 (19)	C(14)-C(15)-C(39)	124.5 (19)
N(2)-C(6)-C(7)	110.8 (28)	C(16)-C(15)-C(39)	118.7 (20)
C(8)-C(9)-N(2)	112.6 (23)	C(1)-C(20)-C(21)	120.1 (21)
N(3)-C(11)-C(12)	107.4 (20)	C(19)-C(20)-C(21)	115.3 (21)
N(3)-C(14)-C(13)	111.4 (20)		
N(4)-C(16)-C(17)	108.7 (24)		
N(4)-C(19)-C(18)	109.7 (20)		

[a] Distance and standard deviation of the refined idealized group S-C(phenyl) distance.

(PPIXDME)(SC_6H_4-*p*-NO_2) (II).[17] In II, the average Fe–N bond distance is 2.064 (18) Å and the iron displacements from the mean porphyrin plane and the N_4 plane are 0.448 and 0.434 Å, respectively. The Fe–S bond distance of 2.298 (3) Å in I is 0.024 Å shorter than the corresponding distance for II.

The Disorder. The diffuse intensity observed in the precession photographs is in the form of circular disks perpendicular to the a^* axis. This scattering is indicative of long-range order in the **a** direction and only short-range order in the **b** and **c** directions; the correlation lengths in the **b** and **c** directions are on the order of 100 Å. The observation that only the $k + l = 2n + 1$ reflections are diffuse implies that the disorder involves a displacement of some structural component by $\mathbf{b}/2 + \mathbf{c}/2$.

Inspection of packing diagrams of the structure suggests the nature of the disorder. The molecules stack with the porphyrin planes approximately perpendicular to the *a* axis. Molecules related by the *a*-glide form a nearly linear column parallel to the **a** direction. The iron atoms and the coordinated thiolate ligands in this column are all displaced to the same side of their porphyrin planes. The sense of the iron atom displacement ascribes a "direction" to each column, with the two inversion-related columns of each unit cell having opposite directions (see Figure 5). The porphyrin ligands in these two columns are related by pseudo-*A*-centering (see Figure 6). For this reason, reversal of the direction of a single column produces a column essentially equivalent to the neighboring columns displaced by $\mathbf{b}/2 + \mathbf{c}/2$. Reversal of the directions of all the columns in any region of the crystal is equivalent to displacement of that region by $\mathbf{b}/2 + \mathbf{c}/2$.

The diffuse nature of the $k + l = 2n + 1$ reflections can thus be attributed to disorder in the orientation of molecular columns; the pattern of column directions exhibited in Figures 5 and 6 is disrupted in the **b** and **c** directions. A disorder of this type results in very little change in the intercolumn interactions because of the pseudo-*A*-centering of the porphyrin ligands and the fact that intercolumn interactions involve primarily the porphyrin phenyl groups; i.e., there is little communication among the Fe–SC_6HF_4 moieties in different columns (see Figure 6).

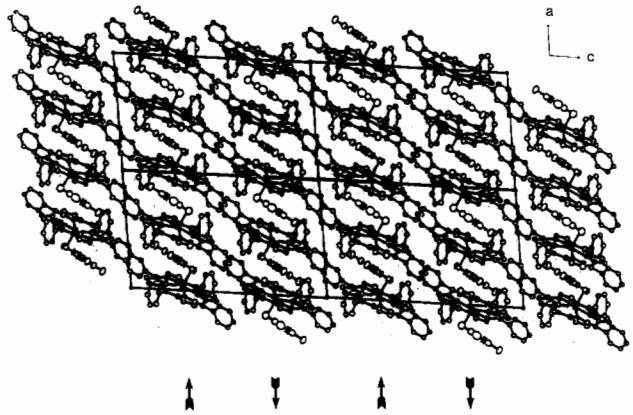

Figure 5. Packing diagram down the *b* axis (*a* axis vertical). The arrows indicate the directions of the iron atom displacement from the porphyrin plane.

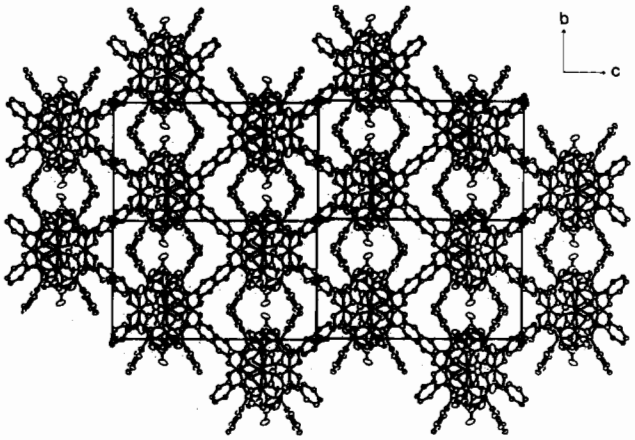

Figure 6. Packing diagram down the *a* axis showing the pseudo-*A*-centering and the intercolumn interactions (*b* axis vertical).

(17) Tang, S. C.; Koch, S.; Papaefthymiou, G. C.; Foner, S.; Frankel, R. B.; Ibers, J. A.; Holm, R. H. *J. Am. Chem. Soc.* **1976**, *98*, 2414.

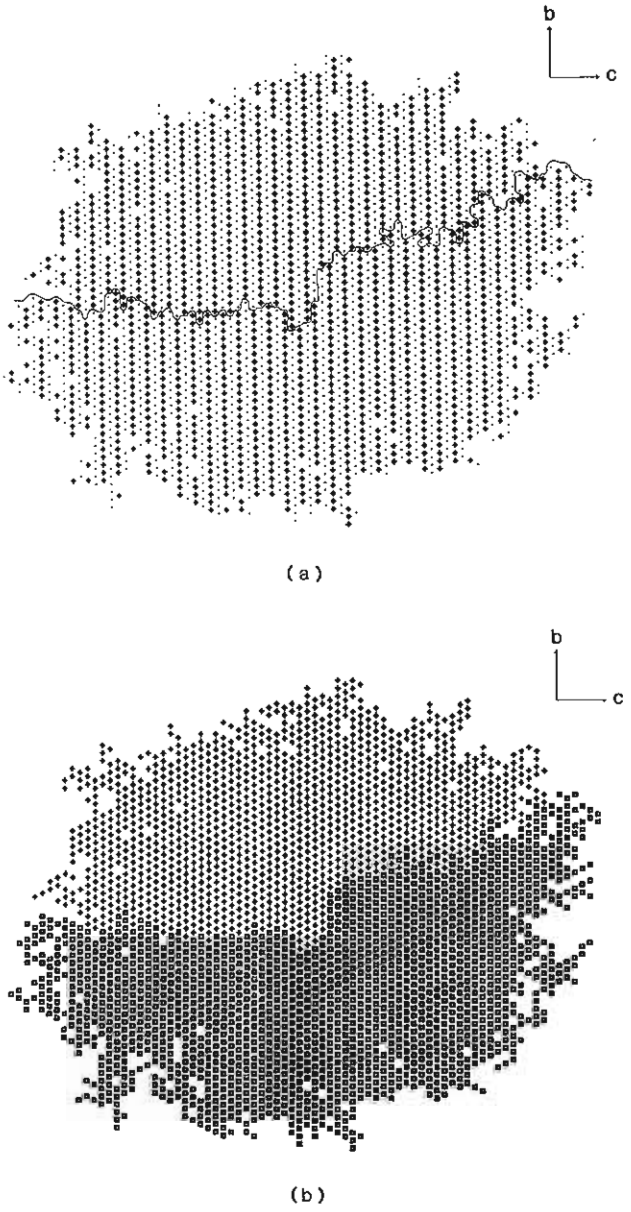

Figure 7. (a) Two-dimensional simulation of crystal growth from a "seed" with one misdirected column. Oppositely directed columns are indicated by dots or plus signs. A boundary line separates the two resulting $P2_1/a$ domains. These domains are related by a translation of $\mathbf{b}/2 + \mathbf{c}/2$. In an ordered domain a molecular column has six nearest neighbors, four related by inversion and two related by translation. (b) Same simulation as in part a but with columns in different domains designated with different symbols, all those in one domain with plus signs and all those in the other with squares.

A two-dimensional disorder analogous to the one described here was reported for a crystalline condensed phosphate, $Na_2P_4O_{11}$.[18] For this material, reflections with l odd consist of diffuse circular disks oriented normal to the c^* axis. Although a detailed analysis was not undertaken, the diffuse scattering was attributed to displacements of random portions of the structure by $\mathbf{c}/2$.

Simulation of Crystal Growth. To illustrate the nature of the short-range order and to examine potential mechanisms for the introduction of the observed disorder, growth of the crystal was modeled in a computer simulation. Since disorder occurs in only the **b** and **c** directions, a two-dimensional simulation was used. Only the interactions of a molecular column with its six nearest neighbors were considered; four of these neighbors are related by inversion and the other two by translation (see Figure 6). New columns were added in random sites on the crystal surface, in directions consistent with those of their neighbors. If the directions of existing columns produced conflicting indications, the direction of the new column was chosen randomly.

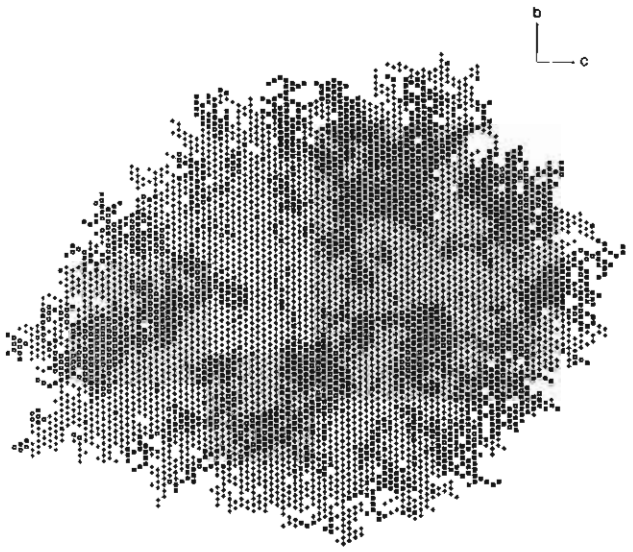

Figure 8. Simulation of crystal growth in which every 20th column is misdirected. The two different $P2_1/a$ domains are shaded with plus signs and squares. This representation illustrates the type of disorder present in the structure of Fe(TPP)(SC_6HF_4).

The consequence of crystal growth from a "seed" with a single misdirected column is depicted in Figure 7. In Figure 7a, oppositely directed columns are represented by dots and plus signs. Inspection of the diagram reveals two $P2_1/a$ domains related by a displacement of $\mathbf{b}/2 + \mathbf{c}/2$. A boundary line has been drawn to separate the two domains. A different representation of the same simulation is depicted in Figure 7b; here the columns of the two domains are indicated with different symbols, all those in one domain with plus signs and those in the other domain with squares. In this representation, the boundary between the domains is obvious. Introduction of a single imperfection results, in this model, in the creation of one and only one new domain. To account for the observed correlation length, therefore, a significant fraction of the columns must be misdirected in either a systematic or random way.

While it is possible to envision various nonrandom mechanisms for the introduction of disorder,[19] in most cases these mechanisms would produce an anisotropic correlation length in the bc plane. No such anisotropy is indicated by the diffuse scattering. A simulation with a random mechanism in which every 20th column added to the crystal is midirected is depicted in Figure 8. The representation used is that depicted in Figure 7b, where different symbols distinguish domains displaced from each other by $\mathbf{b}/2 + \mathbf{c}/2$. The resulting structure has correlation lengths in the **b** and **c** directions of approximately 100 Å, similar to those estimated from the precession photographs (see Figure 1).

Regardless of the actual mechanism for the introduction of the disorder, Figure 8 provides a visualization of the packing disorder that exists in this material. If indeed the disorder results from a random misdirection of newly formed columns, the correlation length would be expected to depend on the

(18) Gryder, J. W.; Donnay, G.; Ondik, H. M. *Acta. Crystallogr.* **1958**, *11*, 38.

(19) For example, mechanisms in which the presence of the particular subsets of the six neighboring columns results in misdirection of the entering column.

temperature at which the crystal formed. A change in correlation length might in turn be reflected in the physical properties of the crystal.

While the type of disorder observed in this compound is unusual, packing disorder in tetraphenylporphinato complexes is relatively common. Several unpublished examples have been observed in this laboratory. In some cases, this disorder occurs because the core of the molecule is insulated from its neighbors by the phenyl substituents, as appears to be true in the present investigation. In other cases, the disorder may arise from inefficient packing due to the perpendicular orientation of the phenyl groups with respect to the porphyrin plane and the relatively rigid geometry of this large ligand. The occurrence of structural equilibria in some ferric tetraphenylporphinato complexes appears to be associated with such "loose packing".

Acknowledgment. This work was supported by a grant from the National Science Foundation (CHE 81-10285) and by the donors of the Petroleum Research Fund, administered by the American Chemical Society. The authors thank Drs. R. M. Sweet, E. Westbrook, and C. Knobler for their suggestions and assistance.

Registry No. I, 90551-70-5.

Supplementary Material Available: Listings of thermal parameters (Table I-S), hydrogen atom positions (Table II-S), porphyrin phenyl group atom positions (Table III-S), and observed and calculated structure factor amplitudes (10 pages). Ordering information is given on any current masthead page.

Contribution from the Department of Chemistry, Louisiana State University, Baton Rouge, Louisiana 70803-1804

Multidentate Ligands Containing 2,2′-Bipyridine and/or Pyridine Moieties: Structural Aspects of Their Octahedral and Pentagonal-Bipyramidal Complexes

GEORGE R. NEWKOME,* VINOD K. GUPTA,[1a] FRANK R. FRONCZEK, and SEBASTIANO PAPPALARDO[1b]

Received July 26, 1983

Multidentate open-chain ligands containing 2,2′-bipyridine and/or pyridine moieties, connected by the CH_2–X–CH_2 bridges in which X is the heteroatom O, S, or N, have been synthesized and characterized. ^{1}H NMR spectral data support the ligand structures. Complexation of these ligands with Co(II), Ni(II), and Cu(II) has been demonstrated. Single-crystal X-ray structural investigations showed a pentagonal-bipyramidal geometry for the Co(II) complex of a pyridine diether ligand (X = O); the five equatorial coordination positions are occupied by the ligand heteroatoms, while two water molecules reside at the axial positions. With the ethereal (X = O) bipyridine ligand the pentagonal-bipyramidal arrangement is retained except that one axial water molecule is replaced by the terminal pyridine group. An octahedral environment around Co(II) or Ni(II) was observed for the thioethers (X = S). The complex $[Ni(C_{24}H_{22}N_4S_2)]Cl_2 \cdot EtOH \cdot 2H_2O$ crystallizes in the triclinic space group $P\bar{1}$. The unit cell dimensions are a = 11.588 (2) Å, b = 11.644 (2) Å, and c = 12.421 (1) Å with α = 114.00 (1)°, β = 99.78 (1)°, γ = 100.98 (1)°, and Z = 2. The $[Co(C_{19}H_{19}N_3O_2)(H_2O)_2]Cl_2$ complex forms monoclinic crystals with the space group $P2_1/c$ and unit cell dimensions a = 13.099 (2) Å, b = 8.052 (1) Å, and c = 20.952 (5) Å, and β = 106.92 (2)° and Z = 4. The complex $[Co(C_{19}H_{19}N_3S_2)Cl]_2[CoCl_4] \cdot 2H_2O \cdot 2MeOH$ crystallizes in the monoclinic space group $P2_1/c$ and has the cell dimensions a = 30.780 (4) Å, b = 9.278 (2) Å, and c = 17.653 (3) Å, and β = 90.80 (1)° and Z = 4.

Introduction

Numerous complexing reagents have been constructed to sequester metal ions, but few have received more attention than those of the pyridine or 2,2′-bipyridine class because of their potential donor abilities.[2] Over the past decade, several ligands, in which an N-heteroaromatic moiety was incorporated within a macrocyclic framework, have been synthesized[3] and their complexation has been demonstrated.[4,5] As a continuation of our work to enhance metal ion selectivity and to better understand the effects of incorporating these binding loci in acyclic vs. cyclic systems, we herein report the synthesis and characterization of the related open-chain polyfunctional ligands **1**. These N-heterocycles were connected by the CH_2–X–CH_2 linkage, in which X is C, O, S, or N, so that the effect of the β atom in subsequent complexation can be evaluated. The 2,2′-bipyridino moiety in **1** has been substituted

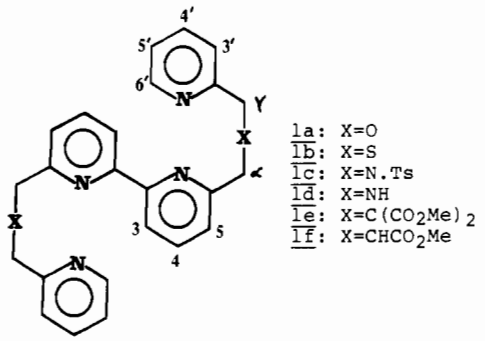

1a: X=O
1b: X=S
1c: X=N.Ts
1d: X=NH
1e: X=C(CO$_2$Me)$_2$
1f: X=CHCO$_2$Me

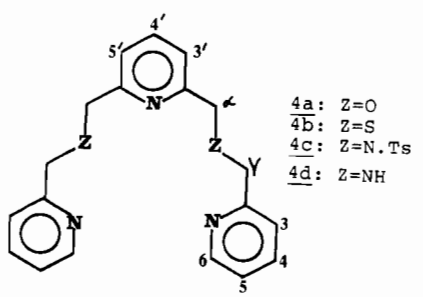

4a: Z=O
4b: Z=S
4c: Z=N.Ts
4d: Z=NH

by a 2,6-pyridino unit to afford the related **4** in order to study the relationship betweeen bi- and monodentate electron-deficient heterearomatics. To evaluate the chelating tendencies

(1) (a) On leave from University of Delhi, Delhi, India (1980–1983). (b) On leave from the Istituto Dipartimentale di Chimica e Chimica Industriale, Universita di Catania, Catania, Italy (1982).
(2) Tomasik, P.; Ratajewicz, Z. In "The Chemistry of Heterocyclic Compounds"; Newkome, G. R., Ed.; Interscience: New York, 1984; Part 6.
(3) Newkome, G. R.; Gupta, V. K.; Sauer, J. D. In "The Chemistry of Heterocyclic Compounds"; Newkome, G. R., Ed.; Interscience: New York, 1984, Part 5.
(4) Newkome, G. R.; Kohli, D. K.; Fronczek, F. R. *J. Chem. Soc., Chem. Commun.* **1980**, 9.
(5) Newkome, G. R.; Kohli, D. K.; Fronczek, F. R.; Hales, B. J.; Case, E. E.; Chiari, G. *J. Am. Chem. Soc.* **1980**, *102*, 7608.

0020-1669/84/1323-2400$01.50/0